Tethered Protein Display Identifies a Novel Kir3.2 (GIRK2) Regulator from Protein Scaffold Libraries

Sviatoslav N. Bagriantsev,[†,#] Franck C. Chatelain,[†,▽] Kimberly A. Clark,[†] Noga Alagem,[⊥] Eitan Reuveny,[⊥] and Daniel L. Minor, Jr.*[,†,‡,§,∥]

[†]Cardiovascular Research Institute, [‡]Departments of Biochemistry and Biophysics, and Cellular and Molecular Pharmacology, [§]California Institute for Quantitative Biomedical Research, University of California, San Francisco, California 94158, United States

[∥]Physical Biosciences Division, Lawrence Berkeley National Laboratory, Berkeley, California 94720, United States

[⊥]Department of Biological Chemistry, Weizmann Institute of Science, Rehovot 76100, Israel

S *Supporting Information*
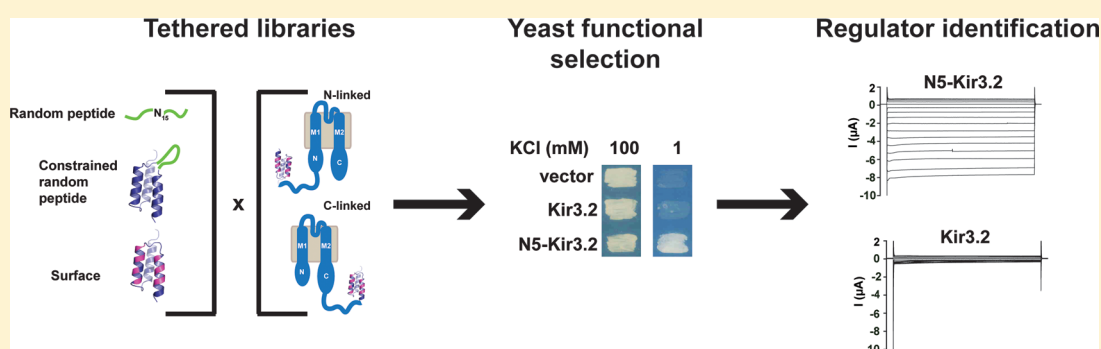
ABSTRACT: Use of randomized peptide libraries to evolve molecules with new functions provides a means for developing novel regulators of protein activity. Despite the demonstrated power of such approaches for soluble targets, application of this strategy to membrane systems, such as ion channels, remains challenging. Here, we have combined libraries of a tethered protein scaffold with functional selection in yeast to develop a novel activator of the G-protein-coupled mammalian inwardly rectifying potassium channel Kir3.2 (GIRK2). We show that the novel regulator, denoted N5, increases Kir3.2 (GIRK2) basal activity by inhibiting clearance of the channel from the cellular surface rather than affecting the core biophysical properties of the channel. These studies establish the tethered protein display strategy as a means to create new channel modulators and highlight the power of approaches that couple randomized libraries with direct selections for functional effects. Our results further underscore the possibility for the development of modulators that influence channel function by altering cell surface expression densities rather than by direct action on channel biophysical parameters. The use of tethered library selection strategies coupled with functional selection bypasses the need for a purified target and is likely to be applicable to a range of membrane protein systems.

KEYWORDS: *Randomized libraries, tethered protein display, channel activation, trafficking, inward rectifier, GIRK*

INTRODUCTION

Ion channels form one of the largest families of signaling proteins in the genome[1,2] and are central to the generation and propagation of bioelectrical signals in the brain, heart, and nervous system.[3] Decades of detailed biophysical studies have provided a deep understanding of the core functional mechanisms of many ion channel classes.[3–5] Nevertheless, despite this rich molecular understanding of functional mechanisms, the development of specific ion channel modulators has lagged and most ion channels lack specific agents that can be used to control function either in vivo or in model systems.[1] This situation underscores the need to develop new molecular entities that can alter channel function as well as new methods for discovering such molecules.[1,4]

Screening of small molecule libraries[1,6,7] and natural peptide toxins[8–10] has provided pathways for discovering novel ion channel regulators, but both approaches remain technically challenging. Combined mutagenesis and selection strategies using a variety of protein scaffolds have been instrumental in developing novel and specific protein based reagents involving a broad range of soluble proteins and domains.[11,12] The use of interaction-based strategies for protein-based modulator development, such as phage display coupled with affinity selection, although demonstrated to work for channels,[13] remains challenging due to difficulties in obtaining suitable quantities of target material. Hence, despite the great power of selection approaches, such strategies have not yet been widely applied to ion channels[14] and there remains a need to develop
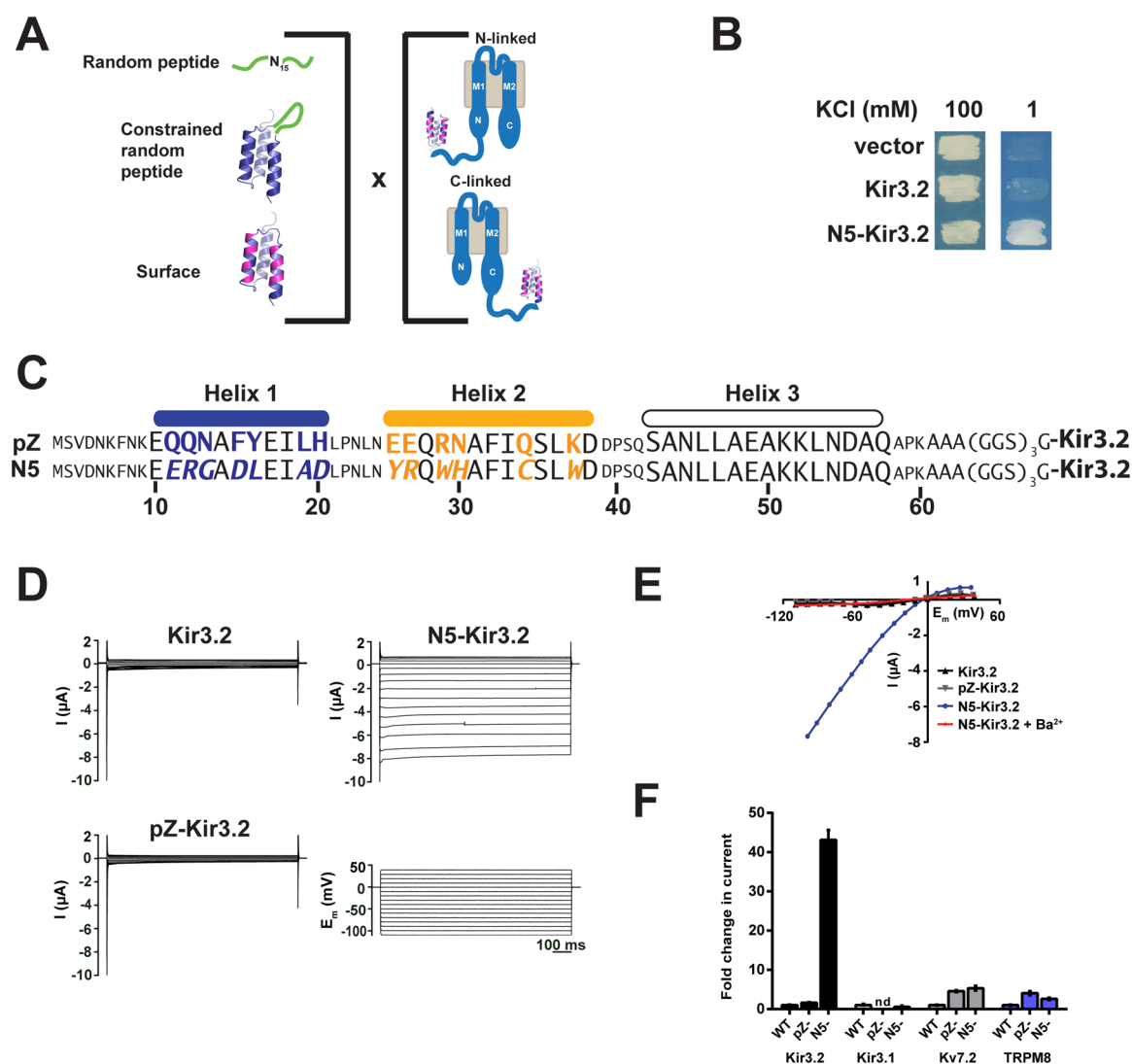
Figure 1. (A) Schematic showing the library display strategy used for identifying Kir3.2 activators. (left) Representations of the random peptide, random peptide (green) constrained by pZ (ribbons), and a pZ surface display library (magenta positions on blue ribbon diagram) were linked to the N- or C-terminal cytoplasmic ends of Kir3.2. (right) Cartoon showing a single Kir3.2 subunit bearing a representative of the N- or C-terminal pZ surface library. (B) Potassium transport complementation assay shows the ability of N5-Kir3.2 to restore growth of the $trk1\Delta trk2\Delta$ yeast on limiting potassium conditions (1 mM KCl). (C) Sequence alignment of pZ and N5. pZ helical segments are shown in large type. Positions randomized in the pZ surface library and the N5 residues at the randomized positions are shown in blue and orange for Helix 1 and Helix 2, respectively. (D) Exemplar two-electrode voltage clamp recordings from *Xenopus* oocytes injected with 3 ng of cRNA for Kir3.2, N5-Kir3.2, and pZ-Kir3.2. Lower right panel shows voltage protocol used for recordings. Currents were evoked by 1 s long step protocol from −110 to 40 mV, in 10 mV increments from a holding potential of 0 mV in 90K. (E) Exemplar current−voltage plots for the indicated constructs recorded in 90K with or without 5 mM $BaCl_2$. (F) Quantification the effects of pZ and N5 on activity of Kir3.2, Kir3.1, Kv7.2, and TRPM8 currents. Kir3.2 were evoked as in (D) and measured at −80 mV. Kv7.2 currents were evoked by 2.5 s long step protocol from −110 to 40 mV in 10 mV increments from a holding potential of −80 mV and measured at +30 mV at 2.4 s. TRPM8 currents were evoked in the presence of 250 μM menthol by a 900 ms long ramp from −110 to 40 mV, from a holding potential of −60 mV, and measured at 30 mV. Data shown as mean ± standard error of the mean (SEM) $n \geq 6$). "nd" indicates not determined.

new strategies to identify and evolve protein-based modulators of channel function.

Functional complementation of potassium transport deficient *Saccharomyces cerevisiae* strains lacking the Trk1p and Trk2p transporters, such as SGY1528,[15,16] has been a fruitful system for the study of a variety of eukaryotic[17−20] and bacterial[21] potassium channels and the characterization of channel interactions with chemical modifiers.[22−24] Here, we use this system to develop a function-based selection that incorporates the basic principles of protein-based selections to search for a protein-based activator of the G-protein coupled inward

rectifier, Kir3.2 (GIRK2).[25] Kir3 channels are a subfamily of inward rectifiers that are deeply involved in cardiovascular, sensory biology, and reward pathways.[26] This channel family has been proposed as an excellent target for development of new compounds aimed at control of cellular excitability.[27,28] By directly coupling library search to function, rather that just binding, we identified a protein A based scaffold termed N5 that activates the channel by affecting its trafficking properties. These results highlight the power of function-based selections for discovering ion channel modulators and emphasize that perturbing properties such as membrane expression may be as
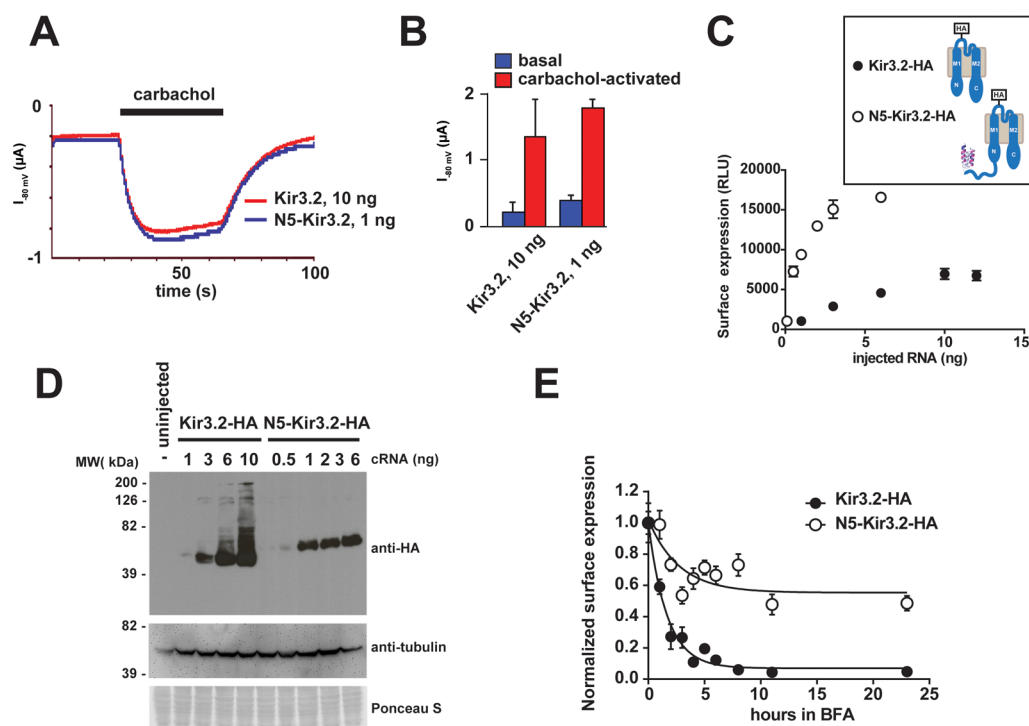
Figure 2. Exemplar recordings (A) and quantification (B) of the effect of 3 μM carbachol on N5-Kir3.2 activity in *Xenopus* oocytes coinjected with 5 ng of mAChR. Data in (B) are mean $\pm$ SD ($n \geq 6$). (C) Quantification of surface expression of HA-tagged Kir3.2 and N5-Kir3.2 as a function of injected cRNA. Data are mean $\pm$ SEM ($n \geq 6$). Inset depicts cartoons of a single subunit of the HA-tagged Kir3.2 and N5-Kir3.2 constructs. (D) Immunoblot analysis of total lysates from oocytes injected with different amounts of cRNA. (E) Quantification of surface expression of N5-Kir3.2-HA in the presence of 15 μM brefeldin A (BFA). Surface fluorescence (SF) measurements (mean $\pm$ SEM, $n \geq 6$) were normalized to the initial fluorescence values and fitted to the single exponential decay equation: SF = $(1 - SF_{plateau}) \exp(-Kt) + SF_{plateau}$, where t is the time in h, $SF_{plateau}$ is the minimal fluorescence, and K is the decay constant.

powerful for controlling channel function as directly targeting the biophysical mechanisms of gating.

■ RESULTS

Rescue of Potassium Transport-Deficient Yeast Identifies a Novel Protein Activator of Mammalian Kir3.2 (GIRK2). We set out to test whether we could use a potassium transport deficient yeast strain, SGY1528 *trk1Δtrk2Δ*,[29] as a platform for selecting protein-based activators of the mammalian inwardly rectifying potassium channel Kir3.2 (GIRK2).[25] Growth of SGY1528 *trk1Δtrk2Δ* under limiting potassium concentrations can be rescued by ectopic expression of a variety of functional potassium channels, making this strain a fruitful system for investigating the properties of a wide range of potassium channel types.[15−20,22−24,30,31] Kir3 channels are usually gated by the interaction of G$_{\beta\gamma}$ subunits with the channel intracellular domains.[32−34] Previous studies demonstrated that different Kir3 family members were incapable of rescuing SGY1528 *trk1Δtrk2Δ* growth but that incorporation of Kir3 activating mutations could rescue the yeast under low potassium conditions.[19,20] Hence, we reasoned that it should be possible to devise a selection scheme to identify exogenous Kir3 activators by looking for a gain-of-function (GOF) effect under low potassium conditions similar to the strategy used to identify activating mutations of Kir3[19,20] and other potassium channels[14,16]

The chance of finding a high affinity activator from a random library is low and compounded by the folding penalties incurred for initial leads.[35] Therefore, we devised a set of strategies to increase the effective concentration[36] of the

potential activator and to preorganize the candidate peptides (Figure 1A). We tested three types of libraries, all of which were tethered to either the Kir3.2 N- or C-terminal cytoplasmic domain by a 13-residue linker (AAAGGSGGSGGSG) to raise the effective concentration relative to the channel. One library type was a simple random 15-mer. We designed a second library in which the random peptide was constrained at both ends because addition of such conformational constraints, which are often included as cysteine pairs that can form a disulfide bond,[35,37−39] can aid in identifying active molecules from random libraries as such constraints lower conformational entropy penalties. Because the intracellular nature of the library and reducing environment of the cytoplasm precluded use of a disulfide constraint, we used the small, well-folded protein Z (pZ), the immunoglobulin-binding domain of the protein A from *Staphylococcus aureus*,[40] as "molecular staple" to constrain a 15 residue library inserted at position Pro22 in the loop between the first two helices of pZ. Finally, in a third library format, we used a "surface remodeling" strategy[41−44] and randomly mutagenized 13 surface residues from Helix 1 and 2 of pZ.

We screened these six libraries to identify candidates that could rescue the SGY1528 potassium transport deficiency under both 1.0 and 0.5 mM potassium conditions and identified ∼50 positive clones that were authentic rescues in yeast (e.g., Figure 1B). Electrophysiological examination of these candidates by two-electrode voltage clamp in *Xenopus* oocytes identified a clone from the pZ surface library, N5 (for Library N, clone 5), in which all 13 surface residues were changed in the parent protein pZ (Figure 1C), that had potent
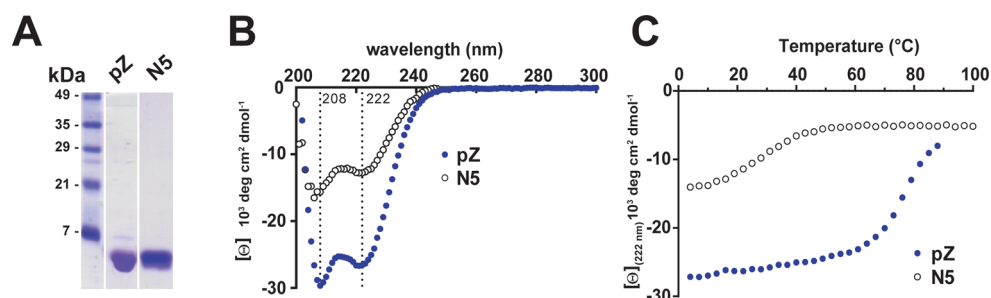
Figure 3. (A) Coomassie-stained SDS-PAGE of purified recombinant pZ and N5. (B) Comparison of pZ and N5 CD spectra at 4 °C. (C) Thermal denaturation of pZ and N5, monitored by CD at 222 nm. CD data were measured in a buffer of 150 mM KCl, 4 mM β-mercaptoethanol, 10 mM phosphate, pH 7.4.

effects on both yeast rescue (Figure 1B) and channel function (Figure 1D and E). Kir3.2 bearing the N5 protein showed robust, barium sensitive, inwardly rectifying currents that contrasted greatly with both wild-type Kir3.2 and Kir3.2 bearing an N-terminal pZ (Figure 1D and E). These data suggest that N5 activates Kir3.2. Although the effect of N5 on Kir3.2 was substantial, N5 had no effect on the related GIRK Kir3.1[45] (Figure 1F). Further tests in which we tethered N5 to the voltage-gated potassium channel Kv7.2 (KCNQ2)[46] or the cold sensitive TRP channel TRPM8[47,48] showed no difference from controls bearing pZ tethered using the identical linkage (Figure 1F) and indicate that the effects of N5 are specific to Kir3.2.

Functional Studies Show That N5 Inhibits Kir3.2 Plasma Membrane Clearance. To gain insight into how N5 stimulates Kir3.2 currents, we used a variety of approaches to investigate the possible mechanisms of N5 action. We first probed whether N5 acted directly as a $G_{\beta\gamma}$-like activator to affect the biophysical properties of the channel by testing whether N5 bearing channels had altered responses to channel activation by G-protein stimulation by $G_{\beta\gamma}$. Coexpression of N5-Kir3.2 with the M2 muscarinic G-protein coupled receptor (mAChR) in *Xenopus* oocytes produced robust carbachol activated currents (Figure 2A and B) that were similar to wild-type when both channels were compared at similar current levels. These data suggest that N5 does not preclude channel activation by $G_{\beta\gamma}$ as might be expected if N5 acted as a $G_{\beta\gamma}$ mimic. Investigation at the level of single channel behavior further supported this idea, as we failed to find any difference from wild-type channels in apparent open probability or in the single channel conductance of N5-Kir3.2 (Figure S1, Supporting Information). Together, these data indicate that N5 is not a $G_{\beta\gamma}$ mimic, does not fundamentally change the biophysical properties of the channel and, hence, must work by some other mechanism.

In comparing $G_{\beta\gamma}$ responses in oocytes, we noticed that N5-tethered Kir3.2 channels displayed a greatly reduced response to $G_{\beta\gamma}$ stimulation when basal currents were larger than ~1 μA at −80 mV in symmetrical potassium conditions. This effect became more prominent at basal current levels >2 μA (Figure S2, Supporting Information). The reduced responses for Kir3.2 were similar to previous reports.[49,50] Notably, we were unable to attain basal current levels > ~ 1 μA with wild-type Kir3.2, even with increasing amounts of injected cRNA (Figure S2C, Supporting Information). The relative ease of obtaining high basal current levels with N5-Kir3.2 led us to consider that N5 might act by affecting Kir3.2 trafficking and channel number at the plasma membrane.

To be able to quantify the effect of N5 on cell surface expression levels, we inserted a hemagglutinin (HA) tag between residues Ile126 and Glu127 in the extracellular loop between the M1 transmembrane segment and the pore helix and used cell surface luminescence assay[51,52] to quantify cell surface expression levels. Inclusion of the HA tag did not perturb the ability of N5 to stimulate Kir3.2 basal current levels (Figure S3, Supporting Information). Quantification of the amount of channels on the cell surface as a function of injected cRNA revealed that N5 caused a 9-fold increase in the amount of N5-Kir3.2-HA at the cell surface relative to wild type Kir3.2-HA when 1 μg of cRNA was injected for each construct, and a 4-fold increase with 6 μg of cRNA (Figure 2C). Immunoblot analysis of whole oocyte lysates demonstrated that the increase in the surface expression was not a consequence of changes in overall protein expression levels (Figure 2D). Thus, N5 appears to act by promoting channel surface expression.

In principle, the abundance of a particular protein at the plasma membrane results from a balance between forward and reverse trafficking.[4,53,54] To investigate further the possible influences of N5 on trafficking, we compared the effect of application of brefeldin A (BFA), an inhibitor of forward trafficking,[55] on the clearance of HA tagged Kir3.2 and N5-Kir3.2 from the oocyte plasma membrane. Continuous treatment of oocytes with BFA resulted in the nearly complete loss of Kir3.2-HA after 8 h due to internalization and recycling. In stark contrast, N5-Kir3.2-HA was much less affected by BFA treatment. Almost 50% of the initial N5-Kir3.2-HA remained on the plasma membrane after 23 h in BFA (Figure 2E), a condition in which essentially all of the Kir3.2-HA signal was lost. Taken together, these data suggest that, rather than act as a $G_{\beta\gamma}$ mimic, N5 stimulates channel basal activity by enhancing surface expression through a mechanism that involves inhibiting clearance of the channel from the plasma membrane.

N5 Contains Multiple Molecular Determinants Essential for Its Activity. We next set out to determine whether there were specific characteristics of N5 or its position relative to the channel that were necessary for function. Because the idea behind the surface display library that generated N5 was to exploit a folded scaffold and yield a protein that retained folded structure, we first asked whether the extensive mutational changes perturbed the structure of the pZ scaffold. To this end, we expressed N5 and pZ in *Escherichia coli*, purified them (Figure 3A), and compared their structural properties by circular dichroism (CD). As expected, the pZ CD spectrum displays the characteristic hallmarks of a predominantly helical protein, having pronounced minima at 208 and 222 nm (Figure 3B).[56] The N5 CD spectrum also had characteristics of helical

815

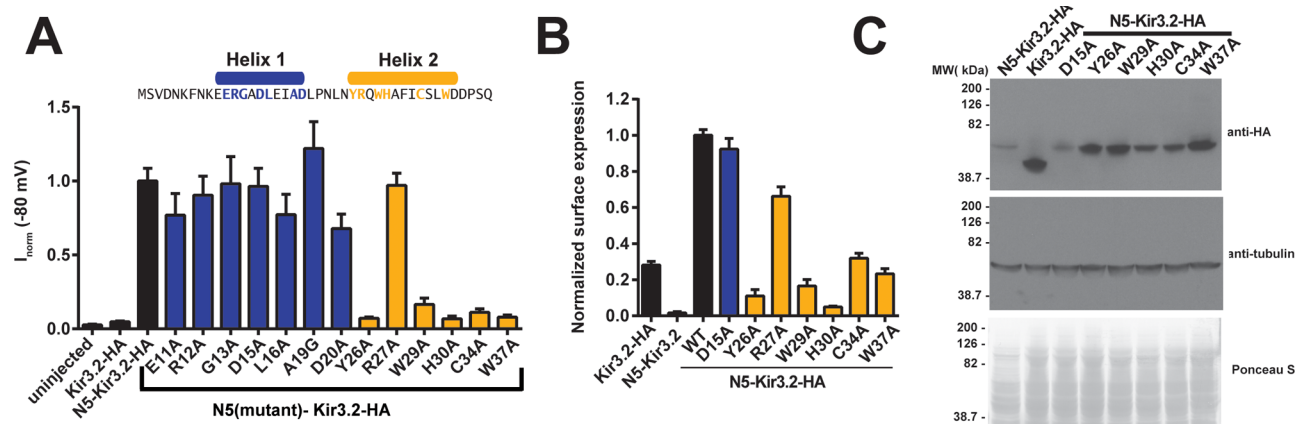dx.doi.org/10.1021/cn5000698 | ACS Chem. Neurosci. 2014, 5, 812−822

Figure 4. Quantification of activity (A), and surface expression (B) of N5-Kir3.2 mutants measured in *Xenopus* oocytes injected with 3 ng of cRNA of each construct. Currents were evoked by a 1 s long step protocol from −110 to 40 mV, in 10 mV increments, from a holding potential of 0 mV in 90K. Surface expression was measured by labeling of the surface of the oocytes with an α-HA antibody. Helix 1 and Helix 2 are indicated by blue and orange, respectively. Data are mean ± SEM ($n \geq 6$). (C) Immunoblot analysis of total lysates from oocytes injected with 3 ng of cRNA of each of the indicated constructs.
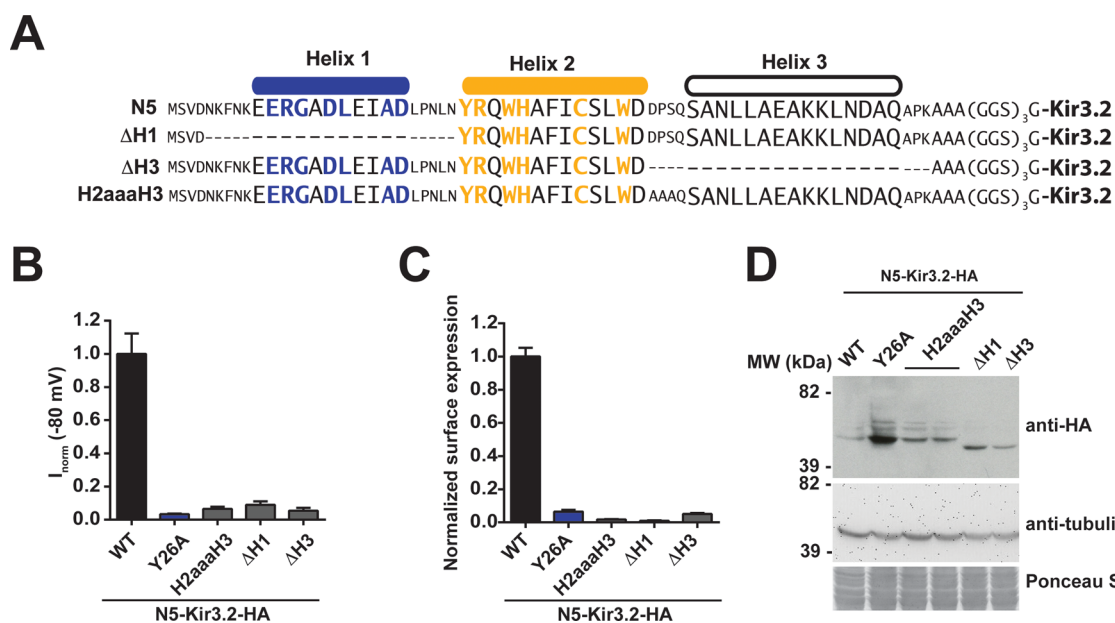

Figure 5. (A) Sequence alignment of wild-type and mutant N5 proteins. Quantification of activity (B) and surface expression (C) of indicated N5-Kir3.2 and mutants measured in *Xenopus* oocytes injected with 3 ng of cRNA of each construct. Currents were evoked by a 1 s long step protocol from −110 to 40 mV, in 10 mV increments, from a holding potential of 0 mV in 90K. Surface expression was measured by labeling of the surface of the oocytes with an α-HA antibody. Data are shown as mean ± SEM ($n \geq 6$). (D) Immunoblot analysis of total lysates from oocytes injected with 3 ng of cRNA for the indicated constructs.

content, but at a substantially reduced intensity relative to pZ (Figure 3B). Thermal denaturation monitored by following the CD signal at 222 nm showed that both pZ and N5 undergo a cooperative loss of secondary structure, the hallmark of a folded protein[57] (Figure 3C). However, N5 has a substantially lower apparent melting temperature (T_m) than pZ, 30 and 77 °C, respectively. Taken together, these data indicate that, despite the extensive changes in sequence, N5 retained the α-helical structure and the folded nature of the parent pZ.

We next used alanine scanning mutagenesis to ask whether any of amino acids at the 13 randomized sites that resulted in the N5 sequence were required for the ability of N5 to stimulate Kir3.2 basal currents and surface expression. Alanine mutations in the seven altered residues of the putative N5 Helix 1 (E11A, R12A, G13A, D15A, L16A, A19A, D20A) failed to

affect the ability of N5 to simulate Kir3.2 activity (Figure 4A). In contrast, alanine substitution in five of the six sites in the putative N5 Helix 2 (Y26A, W29A, H30A, C34A, W37A) dramatically reduced the effects on both channel activity and surface expression (Figure 4A and B). Notably, the loss of stimulation of basal activity and reduced surface expression were not correlated with changes in total channel expression levels (Figure 4C). Hence, these data indicate that there are specific features of N5 responsible for its ability to enhance Kir3.2 function and surface expression and that these elements reside in the putative Helix 2 based on the pZ fold.

Because N5 appears to retain some of the folded characteristics of the parent pZ, we next tested whether changes that would disrupt tertiary structure integrity would affect the ability of N5 to stimulate channel function. Deletion of either the
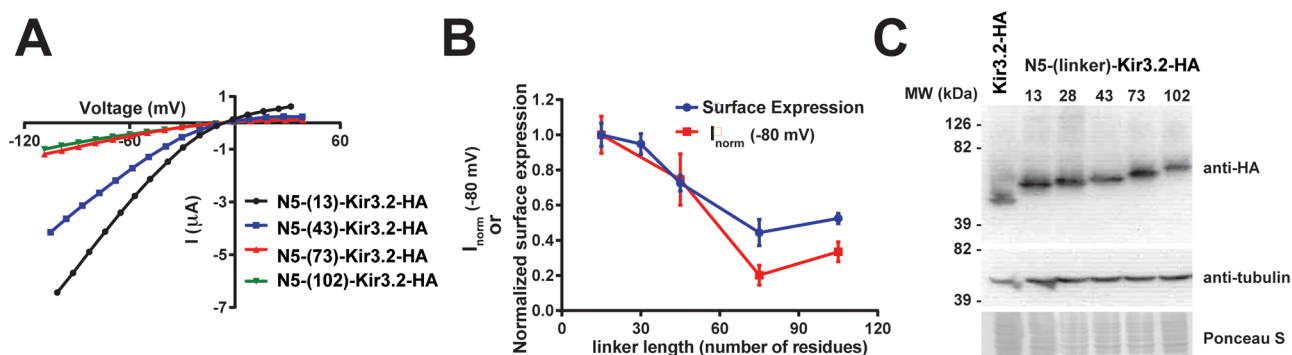
816

dx.doi.org/10.1021/cn5000698 | *ACS Chem. Neurosci.* 2014, 5, 812−822

Figure 6. (A) Exemplar current−voltage plots recorded in oocytes injected with 3 ng of cRNA for the indicated constructs. Currents were evoked by a 1 s long step protocol from −110 to 40 mV, in 10 mV increments, from a holding potential of 0 mV in 90K. (B) Quantification of activity and surface expression of N5$_{mut}$-Kir3.2-HA channels in the oocytes injected with 3 ng of cRNA for each construct. Surface expression was measured by labeling of the surface of the oocytes with an α-HA antibody. Data are mean ± SEM ($n \geq 6$) normalized to N5-Kir3.2-HA. (C) Immunoblot analysis of total lysates from oocytes injected with 3 ng of cRNA for the indicated constructs.
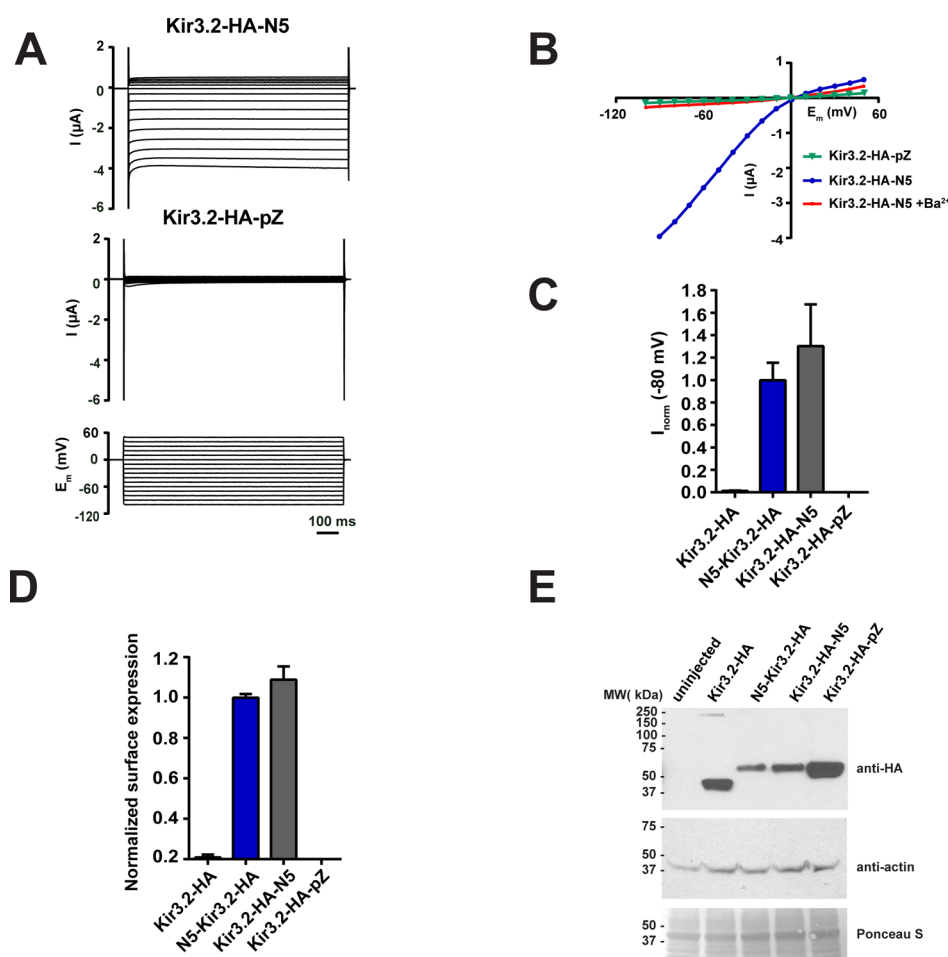

Figure 7. (A) Exemplar two-electrode voltage clamp recordings from *Xenopus* oocytes injected with 3 ng of cRNA for HA-tagged Kir3.2 having N5 or pZ attached to the C-terminus (Kir3.2-HA-N5 and Kir3.2-HA-pZ, respectively). Currents were evoked by a 1 s long step protocol from −100 to 50 mV, in 10 mV increments from a holding potential of 0 mV in 90K. (B) Current−voltage plots recorded in 90K for Kir3.2-HA-pZ and for Kir3.2-HA-N5 with or without the addition of 5 mM BaCl$_2$. (C) Quantification of activity and (D) surface expression of indicated Kir3.2-HA constructs measured in *Xenopus* oocytes injected with 3 ng of cRNA of each construct. Surface expression was measured by labeling of the surface of the oocytes with an anti-HA antibody. Data from at least two experiments were normalized to N5-Kir3.2-HA and shown as mean ± SEM ($n = 8-25$). (E) Immunoblot analysis of total lysates from oocytes injected with 3 ng of cRNA for the indicated constructs.

Helix 1 (ΔH1) or Helix 3 (ΔH3) element (Figure 5A) caused a loss of the ability of N5 to stimulate Kir3.2-HA basal current (Figure 5B) and surface expression (Figure 5C). Similarly, disruption of the turn between H2 and H3 (residues D39-P40-

S41) with a triple alanine replacement (H2aaaH3) (Figure 5A) also resulted a loss of N5 function with respect to its ability to enhance Kir3.2-HA activity and surface expression (Figure 5B and C). These losses of function were equivalent to those seen

in the alanine scan of the H2 positions (cf. Y26A) (Figure 5B and C). None of these changes resulted in loss of protein or degradation of the N5 and linker regions (Figure 5D). Taken together with the biophysical studies of purified N5, these data support the idea that structural integrity of N5 is essential to its ability to stimulate Kir3.2 activity and surface expression. These results demonstrate the utility of using the surface remodeling approach to derive proteins having new function.

N5 Activity Depends on Linker Length. As the other constraint in our library design strategy was covalent tethering to the channel, we next tested whether the linker length made an important contribution to N5 function. To test this parameter, we created a series of constructs that increased the linker length of the flexible tether connecting N5 to the Kir3.2 N-terminus in increments of 15 or 30 residues in the background of the HA-tagged N5-Kir3.2 fusion. Functional tests revealed that the ability of N5 to stimulate Kir3.2 basal currents diminished as the linker became longer (Figure 6A). This loss of current stimulation was concomitant with a loss in the ability of N5 to stimulate surface expression, providing further evidence that the increase in channel basal activity and surface expression effects are linked (Figure 6B). Nevertheless, even with the longest tether tested (102 amino acid), the stimulating effect of N5 on Kir3.2 was still present. Immunoblot analysis confirmed that the long tethers did not cause changes in protein expression levels or altered stability due to proteolysis (Figure 6C). Hence, the dependence of N5 activity on tether length suggests that even though N5 does not act as a $G_{\beta\gamma}$ mimic, its ability to stimulate channel activity by affecting cell surface expression requires some degree of proximity to the channel.

N5 Is Able to Stimulate Channel Activity When Fused to the Kir3.2 C-Terminus. Because N5 was able to stimulate activity even when connected to the channel by a long tether to the channel N-terminus, we next asked whether N5 would stimulate Kir3.2 activity if it were linked to the channel by a completely different covalent linkage than used in the original identification. Attachment of N5 by a covalent linkage to the Kir3.2 C-terminal domain showed potent stimulation of both the macroscopic current (Figure 7A–C) and the relative amount of surface expression (Figure 7D) that were similar to those observed with the original N-terminal linkage. Notably, linking the N5 parent, pZ, to the Kir3.2 C-terminal domain had no effect on channel activity or surface expression (Figure 7A–D), even though the protein expression level of the pZ C-terminal fusion was higher than fusions bearing N5 on either terminus (Figure 7E). These data demonstrate that N5 is able to stimulate Kir3.2 activity and surface expression independent of whether it is attached to the N-terminal (Figure 1D) or C-terminal end of Kir3.2 (Figure 7A). These results contrast those reported for the psychostimulant sorting nexin SNX27, which inhibits Kir3 currents by binding a C-terminal PDZ-binding motif.[58,59] Hence, the N5 mechanism of action appears to be different from that suggested for natural regulators of Kir3 surface expression.

■ DISCUSSION

Development of selective and novel reagents that can be used to alter the function of a target protein of interest poses one of the major challenges of modern biological research. There is an especially acute need for such reagents with respect to ion channels. Even though this protein class comprises >400 signaling proteins of paramount importance in the nervous system,[1,2] most lack any means for selectively altering their functions.[1,4] Ion channels have remained one of the most challenging targets for high throughput screening[1] with potassium channels being especially difficult.[6] A number of recent advances have aided in the prosecution of high-throughput small molecule screens against potassium channel targets, including development of a fluorescent dye that can detect thallium, an ion that permeates many potassium channels,[60−63] and the use of a yeast-based potassium transport strain.[16,22,64,65] Nevertheless, there remains a need to expand the range of systems that can be used to develop new ion channel modulators.

Protein and peptide based reagents from venoms have long been central to the ion channel pharmacology tool kit.[8−10] However, finding such entities from natural sources remains a challenge, as they come from resources that may only be available in small quantities from rare or difficult to handle organisms. In vitro protein evolution and selection approaches using methods such as phage display have contributed greatly to the development of new protein and peptide reagents that bind diverse targets.[11,12] However, such methods have largely been applied to soluble targets. Although purified channels have been used to evolve new toxins by phage display,[13] the availability of high quality target molecules remains a major impediment.

The relationship between current, the functional output of an ion channel, and channel activity relies on three parameters, $I = N\gamma Po$: the number of channels (N), the single channel conductance (γ), and the open probability (Po).[3] Pairing the display of peptide and protein libraries with an assay that relies on functional changes in the target channel, rather than simply binding, offers a powerful way to discover entities that might perturb any or all of these parameters. Here, by exploiting a yeast-based genetic selection that has prior demonstrated utility to identify gain-of-function mutations in a variety of channels,[17−20,23,24,31] we are able to show that it is possible to use tethered peptide and protein display to identify a channel modulator. This tethered activator, N5, is a folded protein based on surface remodeling of the pZ helical bundle scaffold. A variety of lines of evidence demonstrate that rather than affect the core biophysical parameters of the channel, as had previously characterized GOF mutants selected using this system,[17−20,23,24,30,31] N5 perturbs N, the number of channels at the plasma membrane. N5 has this effect by reducing Kir3.2 clearance from the cellular surface (Figure 2E). The ability of N5 to perturb Kir3.2 trafficking requires a folded structure, a set of amino acid changes in a region corresponding to Helix 2 of the parent scaffold, and on its tethering to the N-terminal cytoplasmic domain of the channel.

Basal activity of Kir3 channels (I_{basal}) is thought to be important for the physiological function of the channel in neurons[27,66] and sinoatrial cells,[67] yet the origins of this activity remain a point of contention. Initial studies in *Xenopus* oocytes showed that increased amounts of channel expression augmented I_{basal} and reduced GPCR induced currents.[50] Later studies suggested that most of the basal activity was dependent on $G_{\beta\gamma}$;[68] however, recent studies in atrial myocytes indicate that Kir3 basal currents do not require G-proteins and are agonist independent.[69] No molecular mechanism has been identified to explain Kir3.x basal activity at high channel densities. Our studies of the action of the N5 modulator suggest that the increase of Kir3.2 density in the plasma membrane is sufficient to increase $G_{\beta\gamma}$-independent Kir3.2 basal

currents. This idea is corroborated by the observation that N5 also increases Kir3.2 activity in yeast, which have a $G_{\beta\gamma}$ that inhibits rather than activates Kir3 currents.[70] The effects appear to be selective to Kir3.2, as we found no comparable stimulation of activity when N5 was attached to the related inward rectifier Kir3.1 or to other more distantly related members of the VGIC superfamily.

The exact molecular mechanism of N5 action requires further study. Kir3 channel trafficking is regulated by a number of motifs in the intracellular domains, such as the PDZ-binding motif in the C-tail, which is required for normal trafficking via binding to the sorting nexin SNX27.[58,59] It is possible that N5 interferes with the normal mode of Kir3-SNX27 interaction and modulation to affect the amount of channel on the surface. However, the fact that N5 is equally potent when tagged to either cytoplasmic tail of N5 suggests that it does not act via simply shielding the PDZ-binding domain in the C-terminus, and hence, the N5 mechanism of action appears to be different from that suggested for natural regulators of Kir3 surface expression.

Complementation of potassium transport deficiency in both yeast and bacterial systems has been used to study a diverse set of potassium channels including inward recti-fiers,[15,18–21,23,64,65,71–73] viral potassium channels,[24,74,75] and the K_{2P} channel $K_{2P}2.1$ (TREK-1).[17] The results from our search for a protein-based Kir3.2 activator demonstrate that this general potassium transport rescue framework can be used to develop protein-based ion channel activators. Given the diverse types of potassium channels that function in such genetic selection systems, it should be possible to apply similar strategies to other channel classes to select for molecules that increase channel activity and permit yeast survival or perhaps inhibit channel function and thereby create novel channel modulators. Because potassium homeostasis is a key component of cellular physiology and decreased potassium channel activity is linked to a growing number of channelopathies,[76–78] the ability to rescue potassium channel activity could offer a means for restoring function. Moreover, the ability to express particular channel target robustly in the yeast system should enable the development of small molecule screens against difficult to express targets.

■ METHODS

Molecular Biology. Mouse Kir3.2 (U11859)[25] was cloned into pYES2-MET25 (2 μ, URA3)[18] or pGEMHE/pMO[20] for expression in yeast or for cRNA synthesis, respectively. mAChR was cloned into pGEMHE/pMO. For protein purification, pZ and N5 were cloned into pET28HMT vector (Novagen) as His(x6)-MBP-TEV-pZ(N5) fusions. Cloning was performed using standard molecular biology procedures and verified by sequencing.

Library Construction. Libraries were assembled from synthetic oligonucleotides in which the randomized positions were encoded by the codon NN(G/T) in which N is an equal proportion of each of the four bases. This combination covers all amino acids, eliminates two of the three stop codons, and reduces the truncation frequency in the libraries and assembled by PCR. Design of the pZ surface library followed Nord and co-workers.[41–44] A synthetic gene for protein A having randomized codons (NNG/T) at 13 positions (residues 11, 12, 13, 15, 16, 20, 26, 27, 29, 30, 34, 37) was assembled from synthetic oligonucelotides. All libraries were cloned along with a 13-residue linker (AAAGGSGGSGGSG) as a fusion to Kir3.2.

Yeast Screen. *Saccharomyces cerevisiae* strain SGY1528 (W303, MATα, ade2-1, canl-100, his3–11,15, leu2-3,112, trp1-1, ura3-1, trkl::HIS3, trk2::TRP1)[15] was transformed with each of the mutant libraries, selected on synthetic medium without uracil and methionine

(-Ura-Met) containing 100 mM KCl and transferred by replica plating onto -Ura-Met with 1.0 mM KCl. Positive colonies were grown in liquid -Ura-Met medium with 100 mM KCl; plasmids were isolated, retested, and sequenced. For detailed media compositions, see ref 16. The N5 clone was identified from the pZsurface-Kir3.2 library in which ~48 668 independent transformants were screened.

Electrophysiology. Two-electrode voltage clamp recordings were performed from defolliculated stage V–VI *Xenopus* oocytes 24–72 h after injection, using microelectrodes (0.3–3.0 MΩ) filled with 3 M KCl. Data was acquired using the GeneClamp 500B amplifier controlled by the pClamp software, and digitized at 1 kHz using Digidata 1332A (all from Molecular Devices). Kir3.2, N5-Kir3.2, and N5-Kir3.2 mutant recordings were performed in 90K (90 KCl, 8 NaCl, 1.8 CaCl$_2$, 2 MgCl$_2$, 5 mM HEPES/KOH, pH 7.4). Currents were evoked by a 1 s long step protocol from −110 to 40 mV, in 10 mV increments, from a holding potential of 0 mV. To obtain a baseline background current, measurements were made using the same recording solution supplemented with 5 mM BaCl$_2$. For "Index of activation" experiments, cells were held at −80 mV and perfused sequentially with 90K, 90K supplemented with 3 μM carbachol, 90K, and 90K + 5 mM BaCl$_2$, for periods of 30 s each. "Index of activation" was calculated as $(C − B)/(R − B)$, where C = the maximal carbachol evoked current, R = the maximal 90K current amplitude, and B = the residual leak current in 90K + 5 mM BaCl$_2$. Kv7.2 recordings were performed in ND96 (96 mM NaCl, 2 mM KCl, 1.8 mM CaCl$_2$, 2.0 mM MgCl$_2$, 10 mM HEPES/NaOH, pH 7.4). Currents were evoked by a 2.5 s long step protocol from −110 to 40 mV, in 10 mV increments, from a holding potential of −80 mV. TRPM8 recordings were performed in 120Cs (120 mM CsCl, 2 mM MgCl2, 1 mM EGTA, 10 mM HEPES/CsOH, pH 7.4, supplemented with 250 μM menthol). Currents were evoked by a 1 s long ramp from −150 to +50 mV from a holding potential of −80 mV.

Protein Purification. Proteins were expressed in *E. coli* Rosetta-(DE3)pLysS in 2xYT media at 37 °C. After cell lysis in buffer A (150 mM KCl, 10% sucrose, 1 mM EDTA, 5 mM MgSO$_4$, 100 mM Tris, pH 8.0 supplemented with antiproteases and DNase I), lysates were loaded onto a metal affinity column (Poros 20 MC, Applied Biosystems), washed with Buffer B (250 mM KCl, 10 mM phosphate, pH 7.4), and eluted with buffer C (buffer B supplemented with additional 500 mM KCl, 500 mM imidazole and 4 mM β-mercaptoethanol). Protein eluate was concentrated by centrifugation (Amicon, MWCO 30 kDa) to 1 mL and restored in 14 mL of buffer B. The concentration step was repeated two more times, and protein was restored in 50 mL buffer A supplemented with 4 mM β-mercaptoethanol and subjected to overnight cleavage with TEV protease at room temperature. The reaction was cleared by centrifugation for 10 min at 4000g and loaded onto the Poros 20 MC column. Protein was eluted by buffer C supplemented with 50 mM imidazole, concentrated by centrifugation (MWCO 5,000 kDa) to 600 μL, and purified to homogeneity by size-exclusion chromatography (Superdex 75) in 150 mM KCl, 4 mM β-mercaptoethanol, 10 mM K-phosphate, pH 7.4.

Circular Dichroism Spectroscopy. CD spectra were recorded on the Aviv 215 circular dichroism spectrometer using a 1 mm path length quartz cell at 4 °C in 150 mM KCl, 4 mM β-mercaptoethanol, 10 mM phosphate, pH 7.4. Thermal melts were recorded from 4 to 90 °C at 222 nm. Melting temperature was determined as the inflection point of first derivative of the data.

Immunoblotting. Oocytes were lyzed by repetitive pipetting in a cold buffer of 150 mM NaCl, 1.06 mM KH$_2$PO$_4$, 2.07 mM Na$_2$HPO$_4$, 1% Triton X100, pH 7.4 supplemented with antiproteases for 30 min on ice, and clarified by centrifugation for 15 min at 20 000g. Lysates were treated for 30 min at 50 °C with a sample buffer containing 2% SDS and 2% β-mercaptoethanol, and analyzed by immunoblotting with the HA7 anti-HA mouse monoclonal IgG1 antibodies (Sigma).

Surface Expression. A hemagluttinin tag (Tyr-Pro-Tyr-Asp-Val-Pro-Asp-Tyr-Ala) was inserted between Kir3.2 residues I126 and E127 and was flanked with Ser-Gly spacers (Ile$_{126}$-Ser-Gly-(HA)-Gly-Ser-Glu$_{127}$) to detect channels at the plasma membrane. The surface chemiluminescence assay was done according to ref 52 as follows: 10–

819

dx.doi.org/10.1021/cn5000698 | ACS Chem. Neurosci. 2014, 5, 812–822

12 *Xenopus* oocytes expressing Kir3.2 with an HA tag inserted in the extracellular P1 loop were incubated in 24-well plates in cold ND96 solution (96 mM NaCl, 2 mM KCl, 1.8 mM $CaCl_2$, 2.0 mM $MgCl_2$, 10 mM HEPES/NaOH, pH 7.4) containing 1% bovine serum albumin (ND96/BSA, 2 mL/well) for 30 min on ice, followed by a 30 min incubation with anti-HA antibody (HA7 from Sigma, 1:1000). Oocytes were washed in 5 wells with cold ND96/BSA and then incubated with horseradish peroxidase conjugated goat anti-mouse IgG (Thermo, 1:1000) for 30 min on ice. Following an extensive wash (5 wells with ND96/BSA followed by 7 wells with ND96), each oocyte was placed in a 1.5 mL tube containing 50 μL of the chemiluminescent substrate (ELISA Femto, Thermo). Chemiluminescence was measured immediately for 30 s, using the 20/20 Luminometer (Thermo).

■ ASSOCIATED CONTENT

Ⓢ Supporting Information

Supplementary Figures S1–S3, supplementary methods, and supplementary references. This material is available free of charge via the Internet at http://pubs.acs.org

■ AUTHOR INFORMATION

Corresponding Author
*E-mail: daniel.minor@ucsf.edu.

Present Addresses
#S.N.B.: Department of Cellular and Molecular Physiology, Yale University School of Medicine, New Haven, CT 06510.
▽F.C.C.: Institut de Pharmacologie Moléculaire et Cellulaire, Université de Nice Sophia Antipolis, 06560 Valbonne, France.

Author Contributions
D.L.M. conceived and planned the research, analyzed data, and provided guidance and support throughout. S.N.B. and F.C.C. performed most experiments and molecular cloning. K.A.C. performed protein purification, CD analyses, and cloning. N.A. and E.R. performed single-channel recordings in mammalian cells. D.L.M., S.N.B, and E.R. wrote the paper with contributions from all authors.

Notes
The authors declare no competing financial interest.

■ ACKNOWLEDGMENTS

■ REFERENCES

(1) Bagal, S. K., Brown, A. D., Cox, P. J., Omoto, K., Owen, R. M., Pryde, D. C., Sidders, B., Skerratt, S. E., Stevens, E. B., Storer, R. I., and Swain, N. A. (2013) Ion channels as therapeutic targets: a drug discovery perspective. *J. Med. Chem.* 56, 593–624.

(2) Yu, F. H., and Catterall, W. A. (2004) The VGL-chanome: a protein superfamily specialized for electrical signaling and ionic homeostasis. *Sci. STKE 2004*, re15.

(3) Hille, B. (2001) *Ion Channels of Excitable Membranes*, 3rd ed., Sinauer Associates, Inc., Sunderland, MA.

(4) Isacoff, E. Y., Jan, L. Y., and Minor, D. L., Jr. (2013) Conduits of life's spark: a perspective on ion channel research since the birth of neuron. *Neuron* 80, 658–674.

(5) Catterall, W. A., Raman, I. M., Robinson, H. P., Sejnowski, T. J., and Paulsen, O. (2012) The Hodgkin-Huxley heritage: from channels to circuits. *J. Neurosci.* 32, 14064–14073.

(6) Wulff, H., Castle, N. A., and Pardo, L. A. (2009) Voltage-gated potassium channels as therapeutic targets, *Nature reviews. Drug Discovery* 8, 982–1001.

(7) Dunlop, J., Bowlby, M., Peri, R., Vasilyev, D., and Arias, R. (2008) High-throughput electrophysiology: an emerging paradigm for ion-channel screening and physiology. *Nat. Rev. Drug Discovery* 7, 358–368.

(8) Baron, A., Diochot, S., Salinas, M., Deval, E., Noel, J., and Lingueglia, E. (2013) Venom toxins in the exploration of molecular, physiological and pathophysiological functions of acid-sensing ion channels. *Toxicon 75C*, 187–204.

(9) Klint, J. K., Senff, S., Rupasinghe, D. B., Er, S. Y., Herzig, V., Nicholson, G. M., and King, G. F. (2012) Spider-venom peptides that target voltage-gated sodium channels: pharmacological tools and potential therapeutic leads. *Toxicon* 60, 478–491.

(10) Lewis, R. J., Dutertre, S., Vetter, I., and Christie, M. J. (2012) Conus venom peptide pharmacology. *Pharmacol. Rev.* 64, 259–298.

(11) Lofblom, J., Frejd, F. Y., and Stahl, S. (2011) Non-immunoglobulin based protein scaffolds. *Curr. Opin. Biotechnol.* 22, 843–848.

(12) Boersma, Y. L., and Pluckthun, A. (2011) DARPins and other repeat protein scaffolds: advances in engineering and applications. *Curr. Opin. Biotechnol.* 22, 849–857.

(13) Takacs, Z., Toups, M., Kollewe, A., Johnson, E., Cuello, L. G., Driessens, G., Biancalana, M., Koide, A., Ponte, C. G., Perozo, E., Gajewski, T. F., Suarez-Kurtz, G., Koide, S., and Goldstein, S. A. (2009) A designer ligand specific for Kv1.3 channels from a scorpion neurotoxin-based library. *Proc. Natl. Acad. Sci. U.S.A.* 106, 22211–22216.

(14) Minor, D. L., Jr. (2009) Searching for interesting channels: pairing selection and molecular evolution methods to study ion channel structure and function. *Mol. BioSyst.* 5, 802–810.

(15) Tang, W., Ruknudin, A., Yang, W., Shaw, S., Knickerbocker, A., and Kurtz, S. (1995) Functional expression of a vertebrate inwardly rectifying K^+ channel in yeast. *Mol. Biol. Cell* 6, 1231–1240.

(16) Bagriantsev, S. N., and Minor, D. L., Jr. (2013) Using yeast to study potassium channel function and interactions with small molecules. *Methods Mol. Biol.* 995, 31–42.

(17) Bagriantsev, S. N., Peyronnet, R., Clark, K. A., Honore, E., and Minor, D. L., Jr. (2011) Multiple modalities converge on a common gate to control K2P channel function. *EMBO J.* 30, 3594–3606.

(18) Minor, D. L., Jr., Masseling, S. J., Jan, Y. N., and Jan, L. Y. (1999) Transmembrane structure of an inwardly rectifying potassium channel. *Cell* 96, 879–891.

(19) Sadja, R., Smadja, K., Alagem, N., and Reuveny, E. (2001) Coupling Gbetagamma-dependent activation to channel opening via pore elements in inwardly rectifying potassium channels. *Neuron* 29, 669–680.

(20) Yi, B. A., Lin, Y. F., Jan, Y. N., and Jan, L. Y. (2001) Yeast screen for constitutively active mutant G protein-activated potassium channels. *Neuron* 29, 657–667.

(21) Paynter, J. J., Shang, L., Bollepalli, M. K., Baukrowitz, T., and Tucker, S. J. (2010) Random mutagenesis screening indicates the absence of a separate H(+)-sensor in the pH-sensitive Kir channels. *Channels (Austin)* 4, 390–397.

(22) Bagriantsev, S. N., Ang, K. H., Gallardo-Godoy, A., Clark, K. A., Arkin, M. R., Renslo, A. R., and Minor, D. L., Jr. (2013) A high-throughput functional screen identifies small molecule regulators of temperature- and mechano-sensitive K2P channels. *ACS Chem. Biol.* 8, 1841–1851.

(23) Chatelain, F. C., Alagem, N., Xu, Q., Pancaroglu, R., Reuveny, E., and Minor, D. L., Jr. (2005) The pore helix dipole has a minor role in inward rectifier channel function. *Neuron* 47, 833–843.

(24) Chatelain, F. C., Gazzarrini, S., Fujiwara, Y., Arrigoni, C., Domigan, C., Ferrara, G., Pantoja, C., Thiel, G., Moroni, A., and Minor, D. L., Jr. (2009) Selection of inhibitor-resistant viral potassium channels identifies a selectivity filter site that affects barium and amantadine block. *PloS One 4*, e7496.

(25) Lesage, F., Duprat, F., Fink, M., Guillemare, E., Coppola, T., Lazdunski, M., and Hugnot, J.-P. (1994) Cloning provides evidence for a family of inward rectifier and G-protein coupled K$^+$ channels in the brain. *FEBS Lett. 353*, 37−42.

(26) Hibino, H., Inanobe, A., Furutani, K., Murakami, S., Findlay, I., and Kurachi, Y. (2010) Inwardly rectifying potassium channels: their structure, function, and physiological roles. *Physiol. Rev. 90*, 291−366.

(27) Luscher, C., and Slesinger, P. A. (2010) Emerging roles for G protein-gated inwardly rectifying potassium (GIRK) channels in health and disease. *Nat. Rev. Neurosci. 11*, 301−315.

(28) Lujan, R., Marron Fernandez de Velasco, E., Aguado, C., and Wickman, K. (2014) New insights into the therapeutic potential of Girk channels. *Trends Neurosci. 37*, 20−29.

(29) Ko, C. H., and Gaber, R. F. (1991) TRK1 and TRK2 encode structurally related K$^+$ transporters. *Mol. Cell. Biol. 11*, 4266−4273.

(30) Lai, H. C., Grabe, M., Jan, Y. N., and Jan, L. Y. (2005) The S4 voltage sensor packs against the pore domain in the KAT1 voltage-gated potassium channel. *Neuron 47*, 395−406.

(31) Bichet, D., Lin, Y. F., Ibarra, C. A., Huang, C. S., Yi, B. A., Jan, Y. N., and Jan, L. Y. (2004) Evolving potassium channels by means of yeast selection reveals structural elements important for selectivity. *Proc. Natl. Acad. Sci. U.S.A. 101*, 4441−4446.

(32) Reuveny, E., Slesinger, P. A., Inglese, J., Morales, J. M., Iñiguez-Lluhi, J. A., Lefkowitz, R. J., Bourne, H. R., Jan, Y. N., and Jan, L. Y. (1994) Activation of the cloned muscarinic potassium channle by G protein bg subunits. *Nature 370*, 143−146.

(33) Whorton, M. R., and MacKinnon, R. (2011) Crystal structure of the mammalian GIRK2 K+ channel and gating regulation by G proteins, PIP2, and sodium. *Cell 147*, 199−208.

(34) Whorton, M. R., and MacKinnon, R. (2013) X-ray structure of the mammalian GIRK2-betagamma G-protein complex. *Nature 498*, 190−197.

(35) Clackson, T., and Wells, J. A. (1994) In vitro selection from protein and peptide libraries. *Trends Biotechnol. 12*, 173−184.

(36) Jencks, W. P. (1987) *Catalysis in Chemistry and Enzymology*, Dover Publications, New York.

(37) Luzzago, A., Felici, F., Tramontano, A., Pessi, A., and Cortese, R. (1993) Mimicking of discontinuous epitopes by phage-displayed peptides, I. Epitope mapping of human H ferritin using a phage library of constrained peptides. *Gene 128*, 51−57.

(38) McLafferty, M. A., Kent, R. B., Ladner, R. C., and Markland, W. (1993) M13 bacteriophage displaying disulfide-constrained micro-proteins. *Gene 128*, 29−36.

(39) O'Neil, K. T., Hoess, R. H., Jackson, S. A., Ramachandran, N. S., Mousa, S. A., and DeGrado, W. F. (1992) Indentification of novel peptide antagonists for GPIIb/IIIa from a conformationally constrained phage peptide library. *n Proteins: Struct., Funct., Genet. 14*, 509−515.

(40) Nilsson, B., Moks, T., Jansson, B., Abrahmsen, L., Elmblad, A., Holmgren, E., Henrichson, C., Jones, T. A., and Uhlen, M. (1987) A synthetic IgG-binding domain based on staphylococcal protein A. *Protein Eng. 1*, 107−113.

(41) Nord, K., Gunneriusson, E., Ringdahl, J., Stahl, S., Uhlen, M., and Nygren, P. A. (1997) Binding proteins selected from combinatorial libraries of an alpha-helical bacterial receptor domain. *Nat. Biotechnol. 15*, 772−777.

(42) Nord, K., Gunneriusson, E., Uhlen, M., and Nygren, P. A. (2000) Ligands selected from combinatorial libraries of protein A for use in affinity capture of apolipoprotein A-1M and taq DNA polymerase. *J. Biotechnol. 80*, 45−54.

(43) Nord, K., Nilsson, J., Nilsson, B., Uhlen, M., and Nygren, P. A. (1995) A combinatorial library of an alpha-helical bacterial receptor domain. *Protein Eng. 8*, 601−608.

(44) Nord, K., Nord, O., Uhlen, M., Kelley, B., Ljungqvist, C., and Nygren, P. A. (2001) Recombinant human factor VIII-specific affinity ligands selected from phage-displayed combinatorial libraries of protein A. *Eur. J. Biochem. 268*, 4269−4277.

(45) Kubo, Y., Reuveny, E., Slesinger, P. A., Jan, Y. N., and Jan, L. Y. (1993) Primary structure and functional expression of a rat G-protein-coupled muscarinic potassium channel. *Nature 364*, 802−806.

(46) Wang, H.-S., Pan, Z., Shi, W., Brown, B. S., Wymore, R. S., Cohen, I. S., Dixon, J. E., and McKinnon, D. (1998) KCNQ2 and KCNQ3 potassium channel subunits: Molecular correlates of the M-Channel. *Science 282*, 1890−1893.

(47) McKemy, D. D., Neuhausser, W. M., and Julius, D. (2002) Identification of a cold receptor reveals a general role for TRP channels in thermosensation. *Nature 416*, 52−58.

(48) Peier, A. M., Moqrich, A., Hergarden, A. C., Reeve, A. J., Andersson, D. A., Story, G. M., Earley, T. J., Dragoni, I., McIntyre, P., Bevan, S., and Patapoutian, A. (2002) A TRP channel that senses cold stimuli and menthol. *Cell 108*, 705−715.

(49) Rubinstein, M., Peleg, S., Berlin, S., Brass, D., Keren-Raifman, T., Dessauer, C. W., Ivanina, T., and Dascal, N. (2009) Divergent regulation of GIRK1 and GIRK2 subunits of the neuronal G protein gated K+ channel by GalphaiGDP and Gbetagamma. *J. Physiol. 587*, 3473−3491.

(50) Peleg, S., Varon, D., Ivanina, T., Dessauer, C. W., and Dascal, N. (2002) G(alpha)(i) controls the gating of the G protein-activated K(+) channel, GIRK. *Neuron 33*, 87−99.

(51) Schwappach, B., Zerangue, N., Jan, Y. N., and Jan, L. Y. (2000) Molecular basis for K(ATP) assembly: transmembrane interactions mediate association of a K+ channel with an ABC transporter. *Neuron 26*, 155−167.

(52) Zerangue, N., Schwappach, B., Jan, Y. N., and Jan, L. Y. (1999) A new ER trafficking signal regulates the subunit stoichiometry of plasma membrane K(ATP) channels. *Neuron 22*, 537−548.

(53) Ma, D., and Jan, L. Y. (2002) ER transport signals and trafficking of potassium channels and receptors. *Curr. Opin. Neurobiol. 12*, 287−292.

(54) Schwappach, B. (2008) An overview of trafficking and assembly of neurotransmitter receptors and ion channels (Review). *Mol. Membr. Biol. 25*, 270−278.

(55) Pelham, H. R. (1991) Multiple targets for brefeldin A. *Cell 67*, 449−451.

(56) Berova, N., Nakanishi, K., and Woody, R. W. (2000) *Circular Dichroism: Principles and Applications*, 2nd ed., Wiley-VCH, New York.

(57) Privalov, P. L. (1989) Thermodynamic problems of protein structure. *Annu. Rev. Biophys. Biophys. Chem. 18*, 47−69.

(58) Lunn, M. L., Nassirpour, R., Arrabit, C., Tan, J., McLeod, I., Arias, C. M., Sawchenko, P. E., Yates, J. R., 3rd, and Slesinger, P. A. (2007) A unique sorting nexin regulates trafficking of potassium channels via a PDZ domain interaction. *Nat. Neurosci 10*, 1249−1259.

(59) Balana, B., Maslennikov, I., Kwiatkowski, W., Stern, K. M., Bahima, L., Choe, S., and Slesinger, P. A. (2011) Mechanism underlying selective regulation of G protein-gated inwardly rectifying potassium channels by the psychostimulant-sensitive sorting nexin 27. *Proc. Natl. Acad. Sci. U.S.A. 108*, 5831−5836.

(60) Lewis, L. M., Bhave, G., Chauder, B. A., Banerjee, S., Lornsen, K. A., Redha, R., Fallen, K., Lindsley, C. W., Weaver, C. D., and Denton, J. S. (2009) High-throughput screening reveals a small-molecule inhibitor of the renal outer medullary potassium channel and Kir7.1. *Mol. Pharmacol. 76*, 1094−1103.

(61) Raphemot, R., Kadakia, R. J., Olsen, M. L., Banerjee, S., Days, E., Smith, S. S., Weaver, C. D., and Denton, J. S. (2013) Development and validation of fluorescence-based and automated patch clamp-based functional assays for the inward rectifier potassium channel kir4.1. *Assay Drug Dev. Technol. 11*, 532−543.

(62) Kaufmann, K., Romaine, I., Days, E., Pascual, C., Malik, A., Yang, L., Zou, B., Du, Y., Sliwoski, G., Morrison, R. D., Denton, J., Niswender, C. M., Daniels, J. S., Sulikowski, G. A., Xie, X. S., Lindsley, C. W., and Weaver, C. D. (2013) ML297 (VU0456810), the first

potent and selective activator of the GIRK potassium channel, displays antiepileptic properties in mice. *ACS Chem. Neurosci. 4*, 1278−1286.

(63) Ramos-Hunter, S. J., Engers, D. W., Kaufmann, K., Du, Y., Lindsley, C. W., Weaver, C. D., and Sulikowski, G. A. (2013) Discovery and SAR of a novel series of GIRK1/2 and GIRK1/4 activators. *Bio. Med. Chem. Lett. 23*, 5195−5198.

(64) Zaks-Makhina, E., Kim, Y., Aizenman, E., and Levitan, E. S. (2004) Novel neuroprotective K+ channel inhibitor identified by high-throughput screening in yeast. *Mol. Pharmacol. 65*, 214−219.

(65) Zaks-Makhina, E., Li, H., Grishin, A., Salvador-Recatala, V., and Levitan, E. S. (2009) Specific and slow inhibition of the kir2.1 K+ channel by gambogic acid. *J. Biol. Chem. 284*, 15432−15438.

(66) Luscher, C., Jan, L. Y., Stoffel, M., Malenka, R. C., and Nicoll, R. A. (1997) G protein-coupled inwardly rectifying K+ channels (GIRKs) mediate postsynaptic but not presynaptic transmitter actions in hippocampal neurons. *Neuron 19*, 687−695.

(67) Ito, H., Ono, K., and Noma, A. (1994) Background conductance attributable to spontaneous opening of muscarinic K+ channels in rabbit sino-atrial node cells. *J. Physiol. 476*, 55−68.

(68) Rishal, I., Porozov, Y., Yakubovich, D., Varon, D., and Dascal, N. (2005) Gbetagamma-dependent and Gbetagamma-independent basal activity of G protein-activated K+ channels. *J. Biol. Chem. 280*, 16685−16694.

(69) Kienitz, M. C., Mintert-Jancke, E., Hertel, F., and Pott, L. (2014) Differential effects of genetically-encoded G scavengers on receptor-activated and basal Kir3.1/Kir3.4 channel current in rat atrial myocytes. *Cell. Signalling 26*, 1182−1192.

(70) Peng, L., Mirshahi, T., Zhang, H., Hirsch, J. P., and Logothetis, D. E. (2003) Critical determinants of the G protein gamma subunits in the Gbetagamma stimulation of G protein-activated inwardly rectifying potassium (GIRK) channel activity. *J. Biol. Chem. 278*, 50203−50211.

(71) Grishin, A., Li, H., Levitan, E. S., and Zaks-Makhina, E. (2006) Identification of gamma-aminobutyric acid receptor-interacting factor 1 (TRAK2) as a trafficking factor for the K+ channel Kir2.1. *J. Biol. Chem. 281*, 30104−30111.

(72) Shikano, S., Coblitz, B., Sun, H., and Li, M. (2005) Genetic isolation of transport signals directing cell surface expression. *Nat. Cell Biol. 7*, 985−992.

(73) Paynter, J. J., Andres-Enguix, I., Fowler, P. W., Tottey, S., Cheng, W., Enkvetchakul, D., Bavro, V. N., Kusakabe, Y., Sansom, M. S., Robinson, N. J., Nichols, C. G., and Tucker, S. J. (2010) Functional complementation and genetic deletion studies of KirBac channels: activatory mutations highlight gating-sensitive domains. *J. Biol. Chem. 285*, 40754−40761.

(74) Gebhardt, M., Hoffgaard, F., Hamacher, K., Kast, S. M., Moroni, A., and Thiel, G. (2011) Membrane anchoring and interaction between transmembrane domains are crucial for K+ channel function. *J. Biol. Chem. 286*, 11299−11306.

(75) Balss, J., Papatheodorou, P., Mehmel, M., Baumeister, D., Hertel, B., Delaroque, N., Chatelain, F. C., Minor, D. L., Jr., Van Etten, J. L., Rassow, J., Moroni, A., and Thiel, G. (2008) Transmembrane domain length of viral K+ channels is a signal for mitochondria targeting. *Proc. Natl. Acad. Sci. U.S.A. 105*, 12313−12318.

(76) Cerrone, M., Napolitano, C., and Priori, S. G. (2012) Genetics of ion-channel disorders. *Curr. Opin. Cardiol. 27*, 242−252.

(77) Pattnaik, B. R., Asuma, M. P., Spott, R., and Pillers, D. A. (2012) Genetic defects in the hotspot of inwardly rectifying K(+) (Kir) channels and their metabolic consequences: a review. *Mol. Genet. Metab. 105*, 64−72.

(78) Barel, O., Shalev, S. A., Ofir, R., Cohen, A., Zlotogora, J., Shorer, Z., Mazor, G., Finer, G., Khateeb, S., Zilberberg, N., and Birk, O. S. (2008) Maternally inherited Birk Barel mental retardation dysmorphism syndrome caused by a mutation in the genomically imprinted potassium channel KCNK9. *Am. J. Hum. Genet. 83*, 193−199.